A solar photovoltaic system with ideal efficiency close to the theoretical limit

Yuan Zhao,[1,2] Ming-Yu Sheng,[1,3] Wei-Xi Zhou,[1] Yan Shen,[1] Er-Tao Hu,[1] Jian-Bo Chen,[1] Min Xu,[1] Yu-Xiang Zheng,[1] Young-Pak Lee,[4] David W. Lynch,[5] and Liang-Yao Chen[1,*]

[1]Department of Optical science & Engineering, Fudan University, Shanghai, 200433 China
[2]Department of Optics and Electricity, Shanghai Second Polytechnic University Shanghai, 201209 China
[3]Department of Electronic Information, Shanghai Business School, Shanghai, 200235 China
[4]Department of Physics, Hanyang University, Seoul, South Korea
[5]Department of Physics, Iowa State University, Ames, Iowa, 50011, USA
[*]lychen@fudan.ac.cn

Abstract: In order to overcome some physical limits, a solar system consisting of five single-junction photocells with four optical filters is studied. The four filters divide the solar spectrum into five spectral regions. Each single-junction photocell with the highest photovoltaic efficiency in a narrower spectral region is chosen to optimally fit into the bandwidth of that spectral region. Under the condition of solar radiation ranging from 2.4 SUN to 3.8 SUN (AM1.5G), the measured peak efficiency under 2.8 SUN radiation reaches about 35.6%, corresponding to an ideal efficiency of about 42.7%, achieved for the photocell system with a perfect diode structure. Based on the detailed-balance model, the calculated theoretical efficiency limit for the system consisting of 5 single-junction photocells can be about 52.9% under 2.8 SUN (AM1.5G) radiation, implying that the ratio of the highest photovoltaic conversion efficiency for the ideal photodiode structure to the theoretical efficiency limit can reach about 80.7%. The results of this work will provide a way to further enhance the photovoltaic conversion efficiency for solar cell systems in future applications.

OCIS codes: (040.5350) Photovoltaic; (230.5170) Photodiodes.

References and links

1. R. R. King, D. C. Law, K. M. Edmondson, C. M. Fetzer, G. S. Kinsey, H. Yoon, R. A. Sherif, and N. H. Karam, "40% efficient metamorphic GaInP/GaInAs/Ge multijunction solar cells," Appl. Phys. Lett. **90**(18), 183516 (2007).
2. J. F. Geisz, D. J. Friedman, J. S. Ward, A. Duda, W. J. Olavarria, T. E. Moriarty, J. T. Kiehl, M. J. Romero, A. G. Norman, and K. M. Jones, "40.8% efficient inverted triple-junction solar cell with two independentlymetamorphic junctions," Appl. Phys. Lett. **93**(12), 123505 (2008).
3. W. Guter, J. Schöne, S. P. Philipps, M. Steiner, G. Siefer, A. Wekkeli, E. Welser, E. Oliva, A. W. Bett, and F. Dimroth, "Current-matched triple-junction solar cell reaching 41.1% conversion efficiency under concentrated sunlight," Appl. Phys. Lett. **94**(22), 223504 (2009).
4. S. Kurtz and J. Geisz, "Multijunction solar cells for conversion of concentrated sunlight to electricity," Opt. Express **18**(S1), A73–A78 (2010).
5. W. Shockley and H. J. Queisser, "Detailed balance limit of efficiency of p-n junction solar cells," J. Appl. Phys. **32**(3), 510–519 (1961).
6. A. D. Vos, "Detailed balance limit of the efficiency of tandem solar cells," J. Phys. D. Appl. Phys. **13**(5), 839–846 (1980).
7. C. H. Henry, "Limiting efficiencies of ideal single and multiple energy gap terrestrial solar cells," J. Appl. Phys. **51**(8), 4494–4500 (1980).
8. G. L. Araújo and A. Marti, "Absolute limiting efficiencies for photovoltaic energy conversion," Sol. Energy Mater. Sol. Cells **33**(2), 213–240 (1994).
9. A. Martí and G. L. Araujo, "Limiting efficiencies for photovoltaic energy conversion in multigap systems," Sol. Energy Mater. Sol. Cells **43**(2), 203–222 (1996).
10. A. S. Brown and M. A. Green, "Limiting efficiency for current-constrained two-terminal tandem cell stacks," Prog. Photovolt. Res. Appl. **10**(5), 299–307 (2002).
11. A. Luque and A. Marti, "Increasing the efficiency of ideal solar cells by photon induced transitions at intermediate levels," Phys. Rev. Lett. **78**(26), 5014–5017 (1997).

#156148 - $15.00 USD Received 10 Oct 2011; revised 5 Nov 2011; accepted 6 Nov 2011; published 16 Nov 2011

12. I. Tobías and A. Luque, "Ideal efficiency of monolithic, series-connected multijunction solar cells," Prog. Photovolt. Res. Appl. **10**, 323–329 (2002).
13. S. Kurtz, D. Myers, W. E. McMahon, J. Geisz, and M. Steiner, "A comparison of theoretical efficiencies of multi-junction concentrator solar cells," Prog. Photovolt. Res. Appl. **16**(6), 537–546 (2008).
14. E. D. Jackson, "Areas for improvement of the semiconductor solar energy converter," in *Transactions of the Conference on the Use of Solar Energy* (University of Arizona Press, 1955), p. 122.
15. R. L. Moon, L. W. James, H. A. Vander Plas, T. O. Yep, G. A. Antypas, and Y. Chai, "Multigap solar cell requirements and the performance of AlGaAs and Si cells in concentrated sunlight," in *13th Photovoltaic Specialists Conference* (IEEE, 1978), pp. 859–867.
16. A. Barnett, D. Kirkpatrick, C. Honsberg, D. Moore, M. Wanlass, K. Emery, R. Schwartz, D. Carlson, S. Bowden, D. Aiken, A. Gray, S. Kurtz, L. Kazmerski, M. Steiner, J. Gray, T. Davenport, R. Buelow, L. Takacs, N. Shatz, J. Bortz, O. Jani, K. Goossen, F. Kiamilev, A. Doolittle, I. Ferguson, B. Unger, G. Schmidt, E. Christensen, and D. Salzman, "Very high efficiency solar cell modules," Prog. Photovolt. Res. Appl. **17**(1), 75–83 (2009).
17. M. A. Green and A. Ho-Baillie, "Forty three percent composite split-spectrum concentrator solar cell efficiency," Prog. Photovolt. Res. Appl. **18**(1), 42–47 (2010).
18. R. R. Willey, "Achieving narrow bandpass filters which meet the requirements for DWDM," Thin Solid Films **398–399**, 1–9 (2001).
19. R. Ramaswami and K. N. Sivarajan, *Optical Networks: A Practical Perspective* (Morgan Kaufmann, 1999).
20. L. Y. Chen and D. W. Lynch, "Scanning ellipsometer by rotating polarizer and analyzer," Appl. Opt. **26**(24), 5221–5228 (1987).
21. D. S. H. Chan and J. C. H. Phang, "Analytical methods for the extraction of solar-cell single- and double-diode model parameters from I-V characteristics," IEEE Trans. Electron. Devices **34**(2), 286–293 (1987).

1. Introduction

Great effort has been made recently to improve the photovoltaic efficiency of solar cells [1–4]. The intrinsic characteristics of a single device will limit its photovoltaic response in attempts to achieve high efficiency of photovoltaic conversion in the broad solar-spectrum range [5–13]. The key to overcoming such a physical limitation is to develop a system consisting of a set of solar cells in which the photovoltaic conversion of each cell matches the sub-spectrum of the solar radiation with high conversion efficiency in its sub-region. At present, the most promising approach is to increase the number of P-N junctions by selecting suitable materials [1–3]. In practical device processing to fabricate an integrated tandem multi-junction structure, however, the number of junctions often has been restricted to be less than or equal to three [1–3] due to the critical barrier of lattice mismatch of the materials composed of IV- and III-V-group semiconductors with different lattice constants and energy band structures. For a typical semiconductor with an energy band gap E_g, there will be either no photon absorption when the photon energy $E < E_{g,}$ or high energy loss due to the generation of electron-hole pairs when $E > E_g$ [7]. Therefore, effective photovoltaic conversion with higher efficiency can occur only in a very narrow photon energy region close to E_g, implying that there is significant room to develop a method in which the number of P-N junctions with different energy gaps E_g can be larger than three by using the proper device configuration and technique to achieve the highest photovoltaic conversion efficiency over the entire solar spectrum range. Henry, in his theoretical work, predicted that maximum efficiencies of 37, 50, 56, and 72% can be achieved for cells with 1, 2, 3 and 36 energy gaps, respectively, under the condition of a concentration of 1000 suns [7]. Luque and Marti carried out a calculation predicting that a maximum efficiency of about 63.1% can be achieved, assuming an ideal solar cell with an intermediate-energy band within the principal band gap structure [11], although difficulties, such as the complexity of the device structure and fabrication process and a very high heat dissipation density of the light concentrated on the single integrated cell, will reduce the efficiency in real applications with problems to be solved in the future.

Another useful approach was proposed to use passive optical devices without energy loss to split the solar spectrum into multiple sub-spectrum regions, each matching the energy band structure of the material with higher photovoltaic conversion efficiency in the sub-region [14, 15]. Very high conversion efficiency has been reported recently by using a configuration in which single and multiple junctions of solar cells were used, separated by a dichroic prism which reflects light above 1.4 eV and passes light below 1.4 eV with the element arrangement

#156148 - $15.00 USD Received 10 Oct 2011; revised 5 Nov 2011; accepted 6 Nov 2011; published 16 Nov 2011

of (GaInP/GaAs tandem cell)/ (dichroic prism)/ (Si single junction cell)/(GaInAsP/GaInAs tandem cell) [16,17].

In the present work we study a method in which the main solar radiation in the 300-1800 nm wavelength range is split into 5 sub-spectral regions by using 4 passive dielectric band-pass film filters, matching them optimally to the photovoltaic response of 5 individual photocells with only one P-N junction working in each region. Results with detailed data reduction and analysis show that the method demonstrated in this work, assembling a set of photocells, each with higher photovoltaic response matching a sub-spectrum of the solar spectrum, can achieve higher efficiency. Advanced wavelength-division-multiplexing (WDM) bandpass-filter technology [18,19], which was well developed in the optical communication field in the last decade, can be effectively transferred and applied to the solar energy field. The method reported here provides a way with significant advantage and indicates that more proper materials with suitable band structures can be selected to achieve high photovoltaic conversion efficiency in a narrow solar spectrum region which can be finely tuned by using conventional dielectric band-pass filters with sharp spectral edges to completely avoid optical interference and lattice mismatch effects presented in the usual tandem solar cell. The optical and electric properties of each individual cell containing only one P-N junction to play the role of photovoltaic conversion can be greatly improved. The device structure design and fabrication process can be optimized to enhance the power output by minimizing the internal resistance and other side effects, as well as to reduce the heat dissipation density by dispersing the highly concentrated solar radiation into a set of spectrally-isolated cells.

2. Theoretical models

There are mainly two kinds of theoretical models to predict the efficiency limits of a set of solar cells with different energy gaps assembled in sequence. One is the thermodynamic model, which deals with the intrinsic photovoltaic conversion process of the cell. The other is called the balance model, which is more widely used to refine the conversion process with some assumptions related to the properties of the solar cell [5–13]. The detailed balance model seems to be more suitable to study and determine the efficiency limit of a cell system in which N single-junction solar cells working at room temperature (T_c = 27°C) are spectrally isolated from each other by using spectrum-splitting technology. The equivalent circuit diagram of an ideal single-junction solar cell is shown in Fig. 1. The I-V characteristic of the ith ideal solar cell can be expressed as [5,6]

$$I^i(V^i) = I^i_{ph} - I^i_0[\exp(\frac{qV^i}{kT_C}) - 1], \quad (1)$$

where I^i and V^i are the external current and voltage of the ith solar cell, respectively, q is electron charge and k is Boltzmann's constant. I^i_{ph} and I^i_0 are the photon-generated current and the reverse-saturated current for the ith solar cell, respectively.

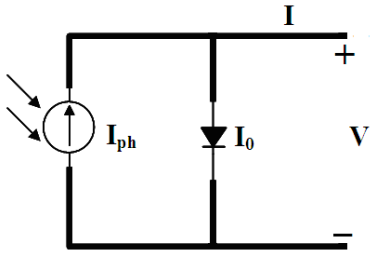

Fig. 1. Equivalent circuit diagram of an ideal single-junction solar cell.

The electron current of the solar cell is generated by absorbing the photons entering the cell. Photons with energy equal to or greater than the band gap E_g are absorbed. Disregarding reflection, we assume that each photon produces only one electron-hole pair and all photon-

#156148 - $15.00 USD Received 10 Oct 2011; revised 5 Nov 2011; accepted 6 Nov 2011; published 16 Nov 2011

generated carriers are collected to produce the power output. The reverse-saturated current arises from the radiative recombination of electron-hole pairs. Assuming that the solar cell is a perfect blackbody in absorbing the radiation and each photon produces only one electron-hole pair in the recombination processes, I^i_{ph} and I^i_0 can be given by [6]

$$I^i_{ph} = q(F_{ph} - F_0), \quad I^i_0 = qF_0, \tag{2}$$

where F_{ph} and F_0 are the number of photons absorbed and radiated per second and can be written as

$$F_{ph} = A\int_{\lambda_n}^{\lambda_{n+1}} N^i_{ph}(\lambda)d\lambda, \quad F_0 = 2A\int_{E_g/h}^{\infty} N^i_0(\nu)d\nu, \tag{3}$$

where A is the effective area of the solar cell, E_g is the bandgap for solar cell, $N^i_{ph}(\lambda)$ and $N_0{}^i(\nu)$ are the absorbed and radiated photon numbers per unit area and per second at wavelengths between λ_n and λ_{n+1} corresponding to the nth sub-spectral window, respectively, and can be written as

$$N^i_{ph}(\lambda) = \frac{C_e E\lambda}{hc}, \quad N^i_0(\nu, T_C) = \frac{2\pi}{c^2}\frac{\nu^2}{\exp(h\nu/kT_C)-1}, \tag{4}$$

where C_e is the energy concentration ratio for the incident solar energy E under 1 sun radiation, c is the velocity of light, ν is the photon frequency and h is Planck's constant. In terms of the I-V characteristic of the ith ideal solar cell, therefore, Eq. (1) can be written as

$$I^i(V^i) = qA\int_{\lambda_n}^{\lambda_{n+1}} \frac{C_e E\lambda}{hc}d\lambda - \frac{4\pi qA}{c^2}\exp(\frac{qV^i}{kT_C})\int_{E_g/h}^{\infty}\frac{\nu^2}{\exp(h\nu/kT_C)-1}d\nu. \tag{5}$$

The output power P^i of the ith ideal solar cell is

$$P^i = I^i V^i. \tag{6}$$

The voltage V^i_m and current I^i_m at the maximum power output condition can be obtained from the condition

$$\frac{\partial P^i}{\partial V^i} = 0. \tag{7}$$

The voltage V^i_m at maximum power output obeys the following equation:

$$[1+\frac{qV^i_m}{kT_C}]\exp(\frac{qV^i_m}{kT_C}) = \frac{h^2c}{4\pi k^3 T_C{}^3}\frac{\int_{\lambda_n}^{\lambda_{n+1}} C_e E\lambda d\lambda}{\sum_{m=1}^{\infty}\frac{1}{m^3}[y^2e^{-y}+2ye^{-y}+2e^{-y}]_{y=mE_g/kT_C}} \tag{8}$$

and the maximum power output $P^i_m = I^i_m V^i_m$ can be expressed as

$$P^i_m = qAV^i_m\int_{\lambda_n}^{\lambda_{n+1}}\frac{C_e E\lambda}{hc}d\lambda - \frac{4\pi qA}{c^2}\frac{k^3T_C{}^3}{h^3}V^i_m\exp(\frac{qV^i_m}{kT_C})\sum_{m=1}^{\infty}\frac{1}{m^3}[y^2e^{-y}+2ye^{-y}+2e^{-y}]_{y=mE_g/kT_C}. \tag{9}$$

The derivation of Eqs. (8) and (9) is in Appendix A.

Thus, the efficiency limit of photovoltaic conversion for assembled solar-cell system can be described as

$$\eta_{\text{model}} = \frac{\sum_{i=1}^{N} P^i_m}{P_{in}} \times 100\%, \tag{10}$$

#156148 - $15.00 USD Received 10 Oct 2011; revised 5 Nov 2011; accepted 6 Nov 2011; published 16 Nov 2011

where P_{in} is the total solar radiation power incident on the solar cell surfaces and can be given as

$$P_{in} = A\int_0^\infty C_e E d\lambda \tag{11}$$

3. Experiment and results

In the experiment, a system containing 5 single-junction cells, two lenses and four filters was configured as shown in Fig. 2. The light beam, simulating a solar spectrum, is transmitted through the first lens and focused onto the first photocell. The filter, which has a spectral window to transmit and reflect light in the short and long wavelength range, respectively, is placed at an angle of 45° in the front of the first photocell. The light which is reflected by the first filter goes to the second set of filters and photocells in sequence. After two reflections by the filters in the optical path, the second lens is used to focus the divergent light onto the

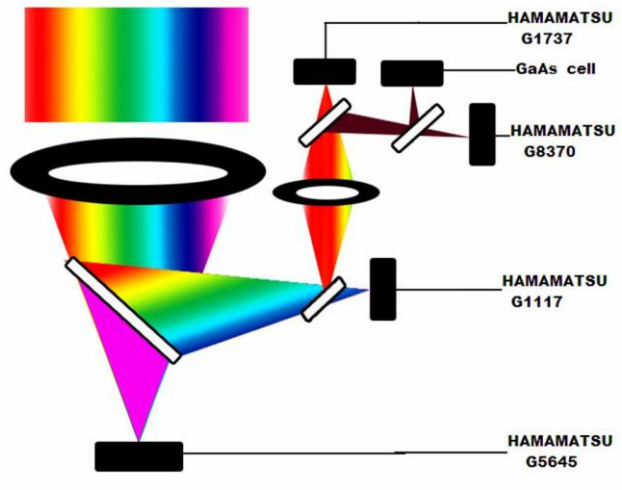

Fig. 2. Schematic diagram of the optical path with five photocells and four filters used in the spectrum-splitting solar photovoltaic conversion system.

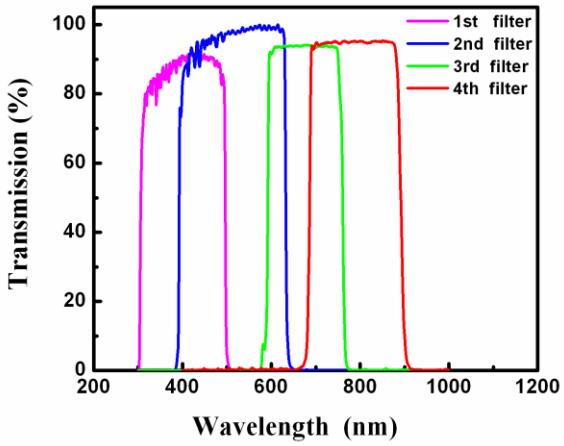

Fig. 3. To match the spectral response of each photocell, four optical film filters have spectral transmission windows of 300-480nm, 400-630 nm, 600-730 nm and 700-870 nm, respectively, as measured by spectroscopic ellipsometry, and are used to divide the solar spectrum into five sub-spectral regions of (I) 300-480 nm, (II) 480-630 nm, (III) 630-730 nm, (IV) 730-870 nm, and (V) 870-1800 nm, respectively.

#156148 - $15.00 USD Received 10 Oct 2011; revised 5 Nov 2011; accepted 6 Nov 2011; published 16 Nov 2011

remaining sets of filters and solar cells. As shown in Fig. 3, the four filters have spectral transmission windows of 300-480 nm, 400-630 nm, 600-730 nm and 700-870 nm, respectively, as measured by spectroscopic ellipsometry [20], and are used to divide the solar spectrum into five sub-spectral regions. There is some degree of spectral overlap between two filters in sequence, resulting in five sub-spectral windows produced by the four filters: (I) 300-480 nm, (II) 480-630 nm, (III) 630-730 nm, (IV) 730-870 nm, and (V) 870-1800 nm, respectively. As shown in Fig. 2, therefore, five photocells with high photovoltaic conversion efficiency peaked at about 470 nm (GaAsP, Hamamatsu G5645), 600 nm(GaAsP, Hamamatsu G1117), 700 nm (GaAsP, Hamamatsu G1737), 850 nm (GaAs, made by the 13th institute of electronics department of China) and 1500 nm (InGaAs, Hamamatsu G8370), respectively, are used to fit optimally in sequence into the I-V sub-spectral regions.

In this study, we use a spectrally-calibrated 1000-W Xe arc lamp as the source in the solar simulator. The spectral mismatch of the solar simulator is less than 10% compared to the standard AM1.5G solar spectrum. The instability of the solar simulator is less than 1% as measured by a standard Oriel silicon cell, satisfying the condition of the standard AM1.5G solar spectrum. The I-V curve for each photocell was measured by Keithley-2400 Source Meter at temperature of 27°C [21] with the results and parameters shown in Fig. 4 and Table 1, respectively.

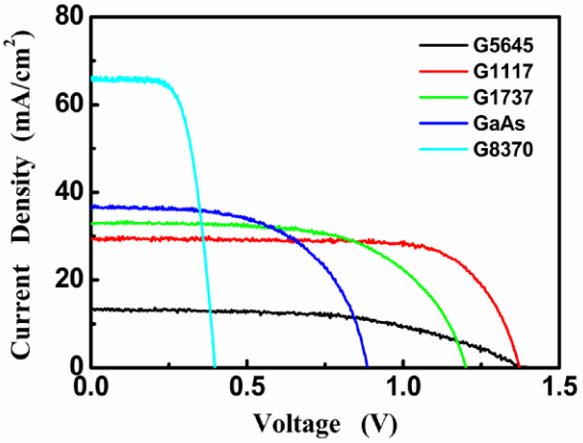

Fig. 4. The I-V curves of five single-junction photocells are measured under the 2.8SUN solar irradiation intensity condition.

Table 1. Parameters extracted from the I-V curves of 5 five single-junction photocells measured under the 2.8SUN solar irradiation intensity condition

Cell	Material	Sub-spectral region (nm)	Effective area size (mm^2)	Short-circuit current density J_{sc} (mA/cm^2)	Open-circuit voltage V_{oc} (V)	Fill Factor (%)	Measured efficiency (%)
G5645	GaAsP	300-480	0.58	13.29	1.39	54.4	3.6
G1117	GaAsP	480-630	29.3	27.54	1.37	74.6	10.1
G1737	GaAsP	630-730	29.3	33.04	1.20	62.0	8.8
GaAs	GaAs	730-870	3.24	36.42	0.89	59.3	6.9
G8370	InGaAs	870-1800	7.0	65.71	0.40	65.8	6.2

In the experiment, the radiation intensity of the solar simulator is varied in the range from 2.4 SUN to 3.8 SUN (AM1.5G). Then the total efficiency η_{exp} of photovoltaic conversion for five solar cells can be measured and analyzed in terms of the I-V curve measured for each cell as

#156148 - $15.00 USD Received 10 Oct 2011; revised 5 Nov 2011; accepted 6 Nov 2011; published 16 Nov 2011

$$\eta_{\exp} = \frac{\sum_{i=1}^{5} I_m^i V_m^i}{P_{in}} \times 100\%, \tag{12}$$

where I^i_m and V^i_m are the output current and voltage of the single solar cell measured under conditions of maximum output power, respectively. When the radiation intensity reaches 2.8 SUN, the highest photovoltaic conversion efficiency of about 35.6% is obtained from the results shown in Fig. 5.

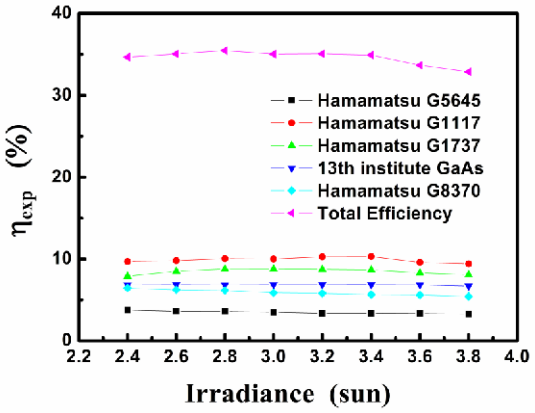

Fig. 5. The measured photovoltaic conversion efficiency changes with the solar irradiation intensity.

In practical applications in which the photocell is irradiated by light from the solar simulator, a certain part of the energy will be lost and converted into thermal power P_{sh} and P_s in the internal shunt resistance R_{sh} and series resistance R_s, respectively, as shown in Fig. 6. Because of the power P_{dio} consumed by the photodiode in the photovoltaic conversion process, the final output power under load, P_{out}, will be smaller than the ideal output power for which $P_{sh} = P_s = 0$.

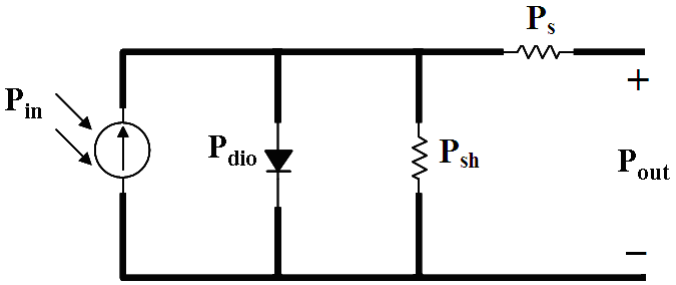

Fig. 6. Schematic diagram to show that the output power will be reduced by the internal shunt and series resistances as the powers P_{sh} and P_s, respectively in the practical application of a solar cell.

Therefore, the output power of the ith single-junction solar cell can be described as

$$P^i_{out} = P^i_{in} - (P^i_{dio} + P^i_s + P^i_{sh}). \tag{13}$$

For an ideal solar cell as shown in Fig. 1, the power consumed by the internal shunt and series resistances should be zero, i.e. the internal shunt and series resistances should reach toward infinity and zero, respectively, in the solar-cell design and manufacturing process to reach the maximal output power of the solar cell with the highest photovoltaic conversion efficiency in application. The output power P^i_{ideal} of the ideal single-junction solar cell can be given as

#156148 - $15.00 USD Received 10 Oct 2011; revised 5 Nov 2011; accepted 6 Nov 2011; published 16 Nov 2011

$$P_{ideal}^{i} = P_{out}^{i} + P_{s}^{i} + P_{sh}^{i}, \tag{14}$$

where the $P_{out,}$ P_s and P_{sh} are

$$P_{out}^{i} = I^{i}V^{i}, \quad P_{s}^{i} = (I^{i})^{2}R_{s}^{i}, \quad P_{sh}^{i} = (V^{i} + I^{i}R_{s}^{i})^{2} / R_{sh}^{i}. \tag{15}$$

The lumped series and shunt resistance R_s and R_{sh}, and the reverse-saturated current for the solar cell I_0 obey the following equations, given in Appendix B:

$$\begin{cases} \dfrac{1}{R_{sh}} = \dfrac{1}{R_{sh0}} - \dfrac{I_0}{V_T}\exp(\dfrac{I_{sc}R_s}{V_T}) \\ R_s = R_{s0} - \dfrac{V_T}{I_0}\exp(-\dfrac{V_{oc}}{V_T}) \\ I_0 = \dfrac{I_{sc}}{\exp(\dfrac{V_{oc}}{V_T}) - \exp(\dfrac{I_{sc}R_s}{V_T})} \end{cases}, \tag{16}$$

where $R^{i}_{sh0} = -(dV/dI)_{V=0}$, $R^{i}_{s0} = -(dV/dI)_{I=0}$ are the shunt and series resistances for the ith solar cell at short- and open-circuit conditions, respectively, and R^{i}_{s} and R^{i}_{sh} are the internal series and shunt resistances of the ith solar cell and can be analyzed in terms of the measured I-V curve [21], and by using Eq. (16), as detailed in Appendix B. For an ideal solar cell, the lumped series and shunt resistance R_s and R_{sh} will be required to equal 0 and ∞ respectively.

Assuming all five single-junction solar cells in the photovoltaic conversion system have the ideal device structure in which $R^{i}_{s} = 0$ and $R^{i}_{sh} = \infty$, the ideal efficiency η_{ideal} of the five-cell system can be described as

$$\eta_{ideal} = \frac{\sum_{i=1}^{5} P_{ideal}^{i}}{P_{in}} \times 100\%, \tag{17}$$

where P^{i}_{ideal} can be analyzed by using Eqs. (14)-(16) under optimal conditions. We find that for solar radiation power in the range of 2.4-3.8 SUN, the spectrally-divided photovoltaic conversion system designed in this work can have a peak conversion efficiency of about 42.7% for a radiation intensity of 2.8 SUN, with the results shown in Fig. 7 and Table 2.

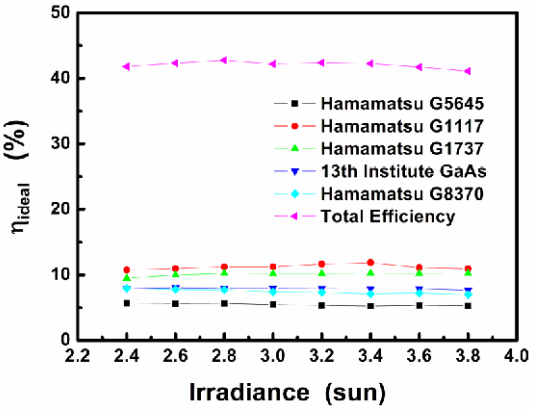

Fig. 7. Photovoltaic conversion efficiency of the spectrally divided system designed in this work to have an optimal efficiency of 42.7% obtained under ideal condition in which $R^{i}_{s} = 0$ and $R^{i}_{sh} = \infty$.

In terms of the detailed-balance model [5–13], the theoretical efficiency limit of the solar cell under 2.8 SUN (solar simulator spectrum) for the spectrally divided solar cell system

#156148 - $15.00 USD Received 10 Oct 2011; revised 5 Nov 2011; accepted 6 Nov 2011; published 16 Nov 2011

given in this work is calculated to reach to about 52.9%, implying that the ratio of the highest photovoltaic conversion efficiency (42.7%) for the solar system with the ideal photodiode structure to the theoretical efficiency limit can reach about 80.7%.

There is room to improve the method and to enhance the photovoltaic conversion efficiency as follows:

(1) There is an optical loss which will reduce the intensity of light incident onto the photocell due to a few percent of transmission loss by the film filters as seen in Fig. 3 and Table 1 and the multiple reflections at the internal and external interfaces of the photocells. This part of the optical loss can be minimized by improving the filter and diode designs and the manufacturing process of the system.

(2) The photovoltaic loss due to the recombination of electron-hole carriers will occur in the photovoltaic conversion process of the solar cell, decreasing the photo-excited photovoltaic current due to defects in the device material and structure. The defects can result in the recombination of electron-hole carriers before conversion into photovoltaic current, reducing the conversion efficiency. This part of the loss can be reduced or overcome by improving the device processing technique.

(3) A certain fraction of the power will be lost and consumed on the internal series and shunt resistances, as seen in Fig. 6. Due to the intrinsic restriction of the photodiode structure, the way to reduce the internal resistance effect in a complicated multi-junction-cell structure is limited. The internal resistance, which will convert a part of solar energy into the heat, can be significantly reduced by improving the device design with suitable processing technique, since there is only one single-junction diode used in the isolated sub-spectral region of the solar radiation spectrum.

(4) The highest photovoltaic conversion efficiency (≥60%) usually occurs only in a narrow region near the direct-energy-band gap of the semiconducting material. For most of the multi-junction solar cell structures, it is still quite difficult to achieve a perfect match between the sub-spectral region of the solar spectrum and optical response region of the solar cell due to the physical limits of the intrinsic optical properties of the semiconductor material and the device structure. By using the method given in this work, however, a proper individual solar cell with higher quantum efficiency can be optimally designed with an optical filter to fit the appropriate sub-spectral region of the solar spectrum, resulting in an overall enhancement of the photovoltaic conversion efficiency. With a multi-junction (>5) solar-cell system with each cell's response matching perfectly its sub-spectral region of the solar spectrum this higher efficiency can be achieved.

Table 2. Measured photovoltaic conversion efficiencies of five photocells in the sub-spectral regions with comparisons to the ideal efficiency under the perfect photo diode structure condition and the efficiency limit calculated by the detailed balance model

Cell	Material	Sub-spectral region (nm)	Solar energy distri-bution (%)	Measured efficiency (η_{exp}, %)	Ideal Efficiency (η_{ideal}, %)	Trans-mission of filter (%)	Ideal efficiency counting filter loss (η^*_{ideal},%)	Efficiency based on detailed balance model (η_{model},%)
G5645	GaAsP	300-480	18.9	3.6	5.7	84.3	6.8	10.7
G1117	GaAsP	480-630	18.5	10.1	11.2	98.3	11.4	11.6
G1737	GaAsP	630-730	16.4	8.8	10.3	94.1	10.9	11.0
GaAs	GaAs	730-870	12.3	6.9	7.9	95.2	8.3	8.3
G8370	InGaAs	870-1800	28.1	6.2	7.7		7.7	11.3
5 cells				35.6	42.7		45.1	52.9

#156148 - $15.00 USD Received 10 Oct 2011; revised 5 Nov 2011; accepted 6 Nov 2011; published 16 Nov 2011

(5) In a highly concentrating solar system, the heat dissipation density of a tandem cell with its multi-junction diode structure will be very high to limit the photovoltaic conversion efficiency in practical applications. By using the spectrum-splitting method with multiple single-junction diodes used in the solar system, the total heat dissipation can be uniformly distributed in each individual photocell to reduce significantly the heat density loaded on the device. This will help to reduce the cost of the solar system under ultra-high light-concentration condition and will improve the performance of the system.

4. Conclusion

In this work, we designed and constructed a solar photovoltaic conversion system consisting of 5 single-junction photocells. Four optical filters were used to divide the solar spectrum into five sub-spectral regions. The single-junction photocell with the highest photovoltaic conversion efficiency in each suitable narrower spectral region was chosen to fit optimally into the bandwidth of each sub-spectral region. Under solar radiation ranging from 2.4 SUN to 3.8 SUN (AM1.5G), the measured peak efficiency for 2.8 SUN radiation reaches about 35.6%, corresponding to an ideal efficiency of about 42.7%, achieved for the photocell system with a perfect diode structure. In terms of the detailed-balance model, the calculated theoretical efficiency limit for the solar system consisting of 5 single-junction photocells can reach about 52.9% under 2.8 SUN (AM1.5G) radiation conditions. Therefore, the ratio of the highest photovoltaic conversion efficiency for the solar cell system with the ideal photodiode structure to the theoretical efficiency limit can reach about 80.7%. The results given in this work will provide a path to further enhance the photovoltaic conversion efficiency of solar systems in future applications.

Appendix A

The derivation of the maximum power output P^i_m for the ith solar cell.

The I-V characteristic of the ith ideal solar cell can be expressed as

$$\mathrm{I}^{\mathrm{i}}(V^i) = qA\int_{\lambda_n}^{\lambda_{n+1}} \frac{C_e E\lambda}{hc} d\lambda - \frac{4\pi qA}{c^2}\exp(\frac{qV^i}{kT_C})\int_{E_g/h}^{\infty} \frac{\nu^2}{\exp(\frac{h\nu}{kT_C})-1} d\nu. \tag{A1}$$

Using the integral formula

$$\int_a^{\infty} \frac{x^2}{\mathrm{e}^{\mathrm{x}}-1} dx = \sum_{m=1}^{\infty} \frac{1}{m^3}[y^2e^{-y} + 2ye^{-y} + 2e^{-y}]_{y=ma}, \tag{A2}$$

the I-V characteristic of the ith ideal solar cell can be expressed as

$$\mathrm{I}^{\mathrm{i}}(V^i) = qA\int_{\lambda_n}^{\lambda_{n+1}} \frac{C_e E\lambda}{hc} d\lambda - \frac{4\pi q}{c^2}\frac{k^3 {T_C}^3}{h^3} A\exp(\frac{qV^i}{kT_C})\sum_{m=1}^{\infty}\frac{1}{m^3}[y^2e^{-y} + 2ye^{-y} + 2e^{-y}]_{\mathrm{y}=mE_g/kT_C}. \tag{A3}$$

The output power of the ith ideal solar cell is written as

$$P^i = qV^i A\int_{\lambda_n}^{\lambda_{n+1}} \frac{C_e E\lambda}{hc} d\lambda - \frac{4\pi q}{c^2}\frac{k^3 {T_C}^3}{h^3} V^i A\exp(\frac{qV^i}{kT_C})\sum_{m=1}^{\infty}\frac{1}{m^3}[y^2e^{-y} + 2ye^{-y} + 2e^{-y}]_{y=mE_g/kT_C}. \tag{A4}$$

The maximum power output can be calculated from

$$\frac{\partial P^i}{\partial V^i} = Aq\int_{\lambda_n}^{\lambda_{n+1}} \frac{C_e E\lambda}{hc} d\lambda - \frac{4\pi q}{c^2}\frac{k^3 {T_C}^3}{h^3} A\left[1+\frac{qV^i}{kT_C}\right]\exp(\frac{qV^i}{kT_C})\sum_{m=1}^{\infty}\frac{1}{m^3}[y^2e^{-y} + 2ye^{-y} + 2e^{-y}]_{y=mE_g/kT_C} = 0 \tag{A5}$$

to obtain the voltage V^i_m and current I^i_m at maximum power output P^i_m, respectively.

#156148 - $15.00 USD Received 10 Oct 2011; revised 5 Nov 2011; accepted 6 Nov 2011; published 16 Nov 2011

Appendix B

Under solar radiation, the I-V characteristic of a practical solar cell shown in Fig.6 is described as

$$\mathrm{I} = I_{ph} - I_0[\exp(\frac{V+IR_s}{V_T})-1] - \frac{V+IR_s}{R_{sh}}. \quad \text{(B1)}$$

where I_{ph} is the photo current of the solar cell, I_0 is the reverse saturated current, R_s and R_{sh} are the lumped series and shunt resistance, respectively, V_T is equal to kT_c/q. Under short-circuit conditions, V=0 and $I=I_{sc}$,

$$I_{sc} = I_{ph} - I_0[\exp(\frac{I_{sc}R_s}{V_T})-1] - \frac{I_{sc}R_s}{R_{sh}}. \quad \text{(B2)}$$

Under open-circuit conditions with I=0 and $V=V_{oc}$,

$$0 = I_{ph} - I_0[\exp(\frac{V_{oc}}{V_T})-1] - \frac{V_{oc}}{R_{sh}}. \quad \text{(B3)}$$

Then

$$I_0[\exp(\frac{V_{oc}}{V_T}) - \exp(\frac{I_{sc}R_s}{V_T})] + \frac{V_{oc}}{R_{sh}} - I_{sc}(1+\frac{R_s}{R_{sh}}) = 0. \quad \text{(B4)}$$

Since $R_s << R_{sh}$, $V_{oc}/R_{sh} << I_{sh}$, Eq. (B4) can be reduced to

$$I_0 = \frac{I_{sc}}{\exp(\frac{V_{oc}}{V_T}) - \exp(\frac{I_{sc}R_s}{V_T})}, \quad \text{(B5)}$$

and thus,

$$\mathrm{I} = I_0 \exp(\frac{V_{oc}}{V_T}) - I_0 \exp(\frac{V+IR_s}{V_T}) + \frac{V_{oc}-V-IR_s}{R_{sh}}. \quad \text{(B6)}$$

Differentiating Eq. (B1) with respect to I,

$$(-R_s - \frac{dV}{dI})[\frac{I_0}{V_T}\exp(\frac{V+IR_s}{V_T}) + \frac{1}{R_{sh}}] = 1. \quad \text{(B7)}$$

Under short-circuit conditions with V = 0, I = I_{sc}, $R_{sh0} = -(dV/dI)_{I=I_{sc}}$, and $R_s << R_{sh0}$, Eq. (B7) can be reduced to

$$\frac{1}{R_{sh}} = \frac{1}{R_{sh0}} - \frac{I_0}{V_T}\exp(\frac{I_{sc}R_s}{V_T}). \quad \text{(B8)}$$

Under open circuit conditions, I = 0, V = V_{oc}, and $R_{s0} = -(dV/dI)_{V=V_{oc}}$, and $[I_0 \exp(V_{oc}/V_T)]/V_T >> 1/R_{sh}$, Eq. (B7) can be reduced to

$$R_s = R_{s0} - \frac{V_T}{I_0}\exp(-\frac{V_{oc}}{V_T}). \quad \text{(B9)}$$

Acknowledgments

This work is supported by the National Science Foundation (NSF) project under contract number 60938004 and by the STCSM project of China (Grant No. 08DJ1400302) and the Shanghai Education Commission Fund (#10YZ213).

#156148 - $15.00 USD Received 10 Oct 2011; revised 5 Nov 2011; accepted 6 Nov 2011; published 16 Nov 2011